JOURNAL OF NANO- AND ELECTRONIC PHYSICS
Vol. **13** No 3, 03003(5pp) (2021)

ЖУРНАЛ НАНО- ТА ЕЛЕКТРОННОЇ ФІЗИКИ
Том **13** № 3, 03003(5cc) (2021)

Preparation and Studies on ZnO Nanoparticles Doped with Ni, Ca and Fe

Srinivasan Kumar[1,*], K.K. Sivakumar[2], Naol Dessalegn Dejene[1], Temesgen Garoma[1], Asagid Tadesse[1]

[1] *Wollega University, Nekemte, Ethiopia*
[2] *Academy of Maritime Education and Training Deemed to be University, India*

(Received 10 January 2021; revised manuscript received 15 June 2021; published online 25 June 2021)

The nanostructures of metal oxides are playing a vital role in determining the characteristics such as magnetic, optical, and electrical properties. In this work, nanostructured ZnO based composites were prepared and their magnetic and optical properties were estimated. The as-prepared composite is composed of $Zn_{0.09}(Ni_{0.05}Ca_{0.05})Fe_{0.01}O$ (ZnNiCaFeO) using co-precipitation method followed by sintering process. To distinguish the role of composites, bare ZnO is also prepared, and its properties are compared with the composite material. Both ZnNiCaFeO) exhibited hexagonal wurtzite structure with the grain size of about 52 and 46 nm, respectively. Hexagonal nanorod structured morphology and the atomic percentage of the as-prepared composites are obtained from the FESEM and EDAX analysis, respectively. UV-Vis absorption spectra of the samples showed absorption peaks at 296 (ZnO) and 288 nm for ZnNiCaFeO NPs. Excitation wavelengths of the composite materials are also estimated from the PL studies. It is noted that composite ZnNiCaFeO exhibited ferromagnetic behavior with the significant magnetization values of 0.34914 emu/g. Thus, the obtained results indicate the composites can be used in soft magnetic application as well as in various optical.

Keywords: Zinc oxide, Co-precipitation, Wurtzite, Optical properties, Ferromagnetic.

DOI: 10.21272/jnep.13(3).03003 PACS numbers: 78.67.Bf, 81.07. – b

1. INTRODUCTION

The enormous applications in various fields such as magnetic, piezoelectric, optical, photocatalysts, gas sensing etc. [1, 2], zinc oxide (ZnO) shows a multifunctional semiconducting metal oxide having a direct energy band gap of 3.37 eV and high binding energy (60 meV). Therefore, it is used. The polar nature of the hexagonal wurtzite lattice allowed to grow various nano sized morphologies such as rods, wires, spindle, belts, stars, and flowers etc. by simply controlling the synthesis conditions [3]. Optical properties of nanocrystalline semiconductors were widely investigated due to its peculiar characteristics such as size and large band gap. Currently, a widespread research has been carried out to explore the effect of doping various metal elements such as Ni^{2+}, $Co^{2+/3+}$ and $Fe^{2+/3+}$ for modifying the electrical, optical, and magnetic properties of various metal oxides [4]. For example, magnetic ferrites ($M_xFe_{3-x}O_4$, where M = Fe, Co, Mn, Ni, or Zn) are versatile nanomaterials having super-paramagnetism and tunable surface properties [5]. Further, optical properties of the above ferrite systems can also be modified due to such doping process [6]. For Miao et al., improve the optical and magnetic properties of the ferrite Zn and Ni doping due to the attribution of defects. Plenty of methods have been reported to synthesis pure and doped ZnO NPs, which can be categorized into either chemical or physical methods such as sol-gel method, solvothermal and co-precipitation method [7-9]. Among them, the co-precipitation method is one of the versatile simple process which is cost effect, giving high yield and homogeneous mixture of reagent precipitates. In addition, it is a simple technique for the synthesis of controlled size and morphology of the metal oxides and metal hydroxides.

In this work, ZnO and Ni, Ca and Fe mixed forms to ZnO matrix, namely, ZNCFO NPs ($Zn_{0.09}(Ni_{0.05}Ca_{0.05})Fe_{0.01}O$) via co-precipitation method has been synthesized and characterized. As prepared samples were subjected to various characterizations such as XRD, FTIR, photoluminescence (PL), VSM, etc.

2. MATERIALS AND METHODS

Zinc (II) nitrate hexahydrate ($Zn(NO_3)_2.6H_2O$), Nickel (II) nitrate hexahydrate ($Ni(NO_3)_2.6H_2O$), Calcium (II) nitrate tetrahydrate ($Ca(NO_3)_2.6H_2O$, Iron (III) nitrate nonahydrate ($Fe(NO_3)_3.9H_2O$) and Sodium hydroxide (NaOH) were purchased from NICE chemicals and used as received.

2.1 Synthesis of ZnNiCaFeO NPs

Pure ZnO nanopowders were synthesized using formerly reported procedures [8]. Briefly, precursor solution of $Zn_{0.09}(Ni_{0.05}Ca_{0.05})Fe_{0.01}O$ NPs (ZnNiCaFeO), was obtained using co-precipitation process Thereafter, the precipitate powder was washed several times using double distilled water followed by ethanol solvents until reaching the pH of the washed solution to neutral condition. After washing, the collected powder was dried at 120 °C for 6 h in vacuum oven. Eventually, the obtained product was calcinated at 700 °C for 5 h in a muffle furnace at air medium to get pure ZnO and ZnNiCaFeO samples.

2.2 Characterization Technique

ZnO and ZnNiCaFeO NPs were characterized by X-ray diffractometer (model: X'PERT PRO PANalytical)

* sivakumarkk@ametuniv.ac.in
The results were presented at the International Conference on Innovative Research in Renewable Energy Technologies (IRRET-2021)

recorded in the range of 20-80° with the monochromatic wavelength of 1.54 Å. Morphological studies were performed in (Carl Zeiss Ultra 55 FESEM) with EDAX (model: Inca) model. FT-IR spectra of the samples were recorded in the range of 400-4000 cm^{-1} by using Perkin-Elmer spectrophotometer. Raman spectra were recorded using Burker RFS 25 spectrometer. The absorption spectra of the samples were carried in the range between 200 and 1100 nm by Lambda 35 spectrometer. The vibrating sample magnetometer were recorded 2.17 Tesla using as a Model 7404.

3. RESULTS AND DISCUSSION

X-ray diffraction patterns of ZnO and ZnNiCaFeO NPs recorded are shown in Fig. 1a. The characteristic peaks obtained at angle of (2θ) of 31.8, 34.6, 36.3, 47.6, 56.6, 62.9, 66.4, 67.9 and 69.1° are corresponding to (100) (002) (101) (102) (110) (103) (200) (112) and (201) lattice planes of the ZnO NPs. The standard diffraction peaks confirmed the hexagonal wurtzite structure of ZnO NPs with space group p63mc, which is well matched with the JCPDS data (Card No: 79-2205). In order to examine the effect of ZnO on ZnNiCaFeO composite on the structure is confirmed from an enlarged version of the XRD pattern between 34 to 35° (Fig. 1b). In case of ZnNiCaFeO NPs, a new phase has emerged an angle between 37 and 43.1° corresponding to Fe_3O_4 along (311) and (400) planes [10], further, the unreacted Fe^{3+} present in the final composition is also evidenced from Fig. 1c, d.

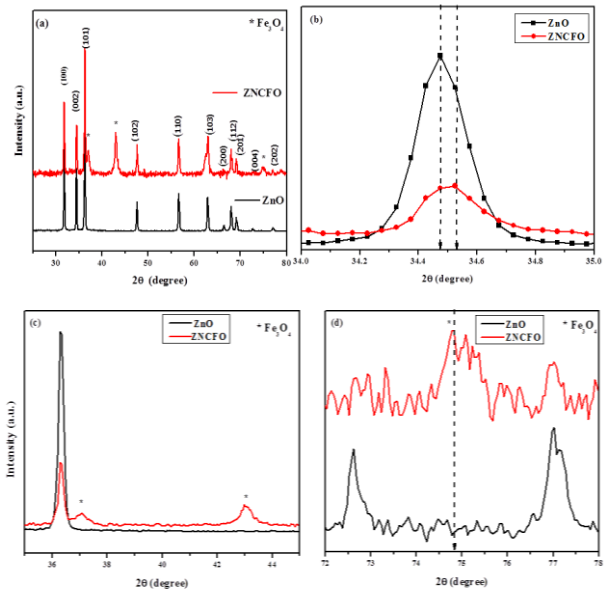

Fig. 1 – X-ray diffraction pattern of (a) ZnO and ZNCFO NPs, (b) the doping-induced peak shift for NPs, (c), (d) enhanced XRD spectra of Fe_3O_4 secondary peaks

The lattice constants 'a' and 'c' of the wurtzite structure of ZnO NPs is calculated by using the relation,

$$\frac{1}{d^2} = \frac{4}{3}\left(\frac{h^2 + hk + k^2}{a^2}\right) + \frac{l^2}{c^2}, \qquad (1)$$

with the first order approximation ($n = 1$) for the (100) plane. The lattice constant 'a' is obtained through the relation $a = \frac{\lambda}{\sqrt{3}\sin\theta}$ and lattice constant 'c' is derived for the plane (002) by the relation $c = \frac{\lambda}{\sin\theta}$. The calculated values of 'a' and 'c' are 3.2472 and 5.2024 Å for ZnO NPs whereas ZnNiCaFeO NPs have 3.2282 and 5.1982 Å, respectively.

The calculated values showed decrease in lattice constants due to the effect of Fe atoms trapped in the non-equilibrium position are shifted to a more equilibrium position.

$$V = \frac{\sqrt{3}a^2c}{2} = 0.866a^2c. \qquad (2)$$

The unit cell volumes calculated by the above relation are found to be 47.5050 $Å^3$ and 47.4959 $Å^3$ for pure ZnO and ZnNiCaFeO NPs, respectively. The unit cell volume in ZnNiCaFeO also decreases with the effect of Ni, Ca and Fe ions in ZnO matrix.

The effect of doping on bond length of Zn–O is calculated by using the relation,

$$L = \sqrt{\frac{a^3}{3} + \left(\frac{1}{2} - u\right)^2 c^2}, \qquad (3)$$

where 'a' and 'c' are lattice parameters and 'u' positional parameter which is measured from the amount by which each atom is displaced with respect to the next along the c-axis. The parameter 'u' can be calculated by the formula

$$u = \left(\frac{a^2}{3c^2}\right) + 0.25 \qquad (4)$$

showed a strong correlation between the c/a ratio and 'u'. The c/a ratio decreases with increasing 'u' in such a way that those four tetrahedral distances remain nearly constant through a distortion of tetrahedral angels due to the long-range polar interaction. The c/a ratio decreases in the ZnNiCaFeO NPs as compared to that of the ZnO NPs.

The bond length of pure ZnO and ZnNiCaFeO NPs are 1.9758 and 1.9756 Å, respectively, and the change in bond length is attributed to high ionic radius of Fe^{3+}. In hexagonal wurtzite structure, the metal and oxygen ion in ZnO faces directly positioned in "c" axis, but for the "a" and "b" axis, the structure contains only oxygen ions facing each other. Therefore, oxygen ion is diagonally connected to the metal ion so that the variation is significant in "c" axis but not in "a" axis [11].

Debye Scherrer's relation [8] calculates the average crystalline size of the sample. The average crystallite sizes 52 and 46 nm for ZnO and ZnNiCaFeO NPs, respectively. The reduction in the particles size is mainly due to the distortion in the host ZnO lattice due to the foreign impurity, i.e., Ni^{2+}, Ca^{2+} and Fe^{3+} ions, which decrease the nucleation and subsequent growth rate of ZnO NPs.

The surface morphology of the ZnO and ZnNiCaFeO NPs are observed from the FESEM analysis at different magnifications (Fig. 2a-d). The FESEM image

clearly shows the uniform size of the NPs in the order of nanometer size of below 200. The ZnO NPs are exhibits hexagonal spherical like structure with even grain sizes. Whereas in the case of ZnNiCaFeO composite, there are nanorod shaped particles overlapped on the hexagonal structure of the ZNO confirmed the presence of the other compounds which is also evidenced from the EDAX spectrum.

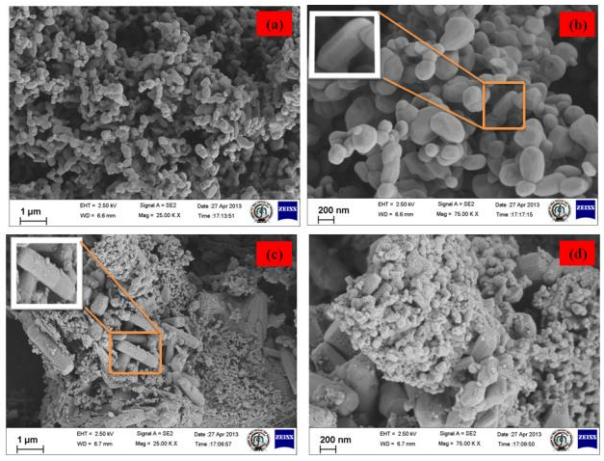

Fig. 2 – FESEM image with low and high resolution for: (a, b) ZnO NPs, (c, d) ZNCFO NPs

The chemical compositional analysis of ZnO and ZnNiCaFeO NPs carried out using EDX spectra are shown in Fig. 3a and b, respectively. From the EDX analysis, the amounts of Zn, Ni, Ca, Fe and O present in the pure ZnO and ZnNiCaFeO samples are estimated. In the composite sample, the concentration of Ni, Ca and Fe are found to be 20.16, 21.31 and 2.02 %, respectively. In the ZnO and ZnNiCaFeO NPs, the chemical composition of Zn and O are found as (52.44 % and 47.56 %) and (24.69 % and 31.82 %), respectively, which confirmed the effective compound for formation during the synthesis process.

Further, the b band formation of the composite and the pure ZnO samples are evidenced from the FT-IR spectral analysis. Fig. 4 showed FT-IR spectra of the ZnO and ZnNiCaFeO samples; the spectra showed the peaks around at 3443 and 3418 cm^{-1} which correspond to O–H stretching vibration, whereas the peaks at 1633 $cm^{-1}$and 1618 cm^{-1} are related to O–H bending vibration [12] of the prepared samples. In the ZnO sample, the Zn–O band was observed at 445 cm^{-1} [11]. However, the Zn–O band is shifted to 620-550 cm^{-1} range in the ZnNiCaFeO sample confirmed the presence of stabilized Ni^{2+} and Ca^{2+} in the ZnO matrix, whereas Zn^{2+} prefers tetrahedral sites because of its ability to form covalent bonds.

The relation between the absorption coefficient (α) and the incident photon energy ($h\nu$) can be written as

$$\alpha h\nu = A\left(h\nu - E_g\right)^n, \qquad (5)$$

where E_g is the optical bandgap, A is the constant and the exponent n depends on the type of transition. The n = 1/2 for allowed direct transition, 2 for allowed indirect transition 3/2 and 3 for forbidden direct and indirect transitions, respectively [13]. The reduction in particle size results in increase of surface/volume ratio. The surface atom has lower coordination number and atomic interaction, which increases the highest valence band energy and decreases the lowest unoccupied conduction band energy.

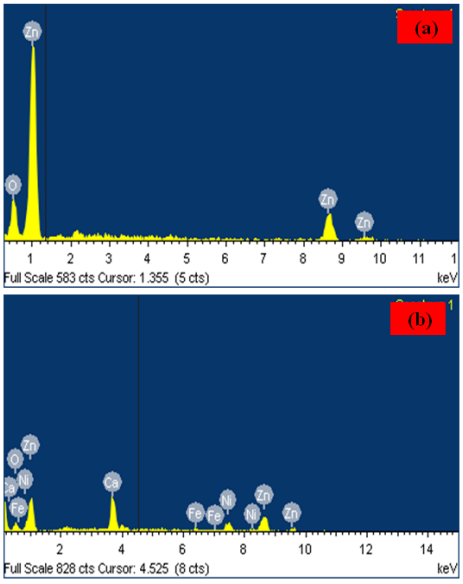

Fig. 3 – EDX spectra of a) ZnO and b) ZNCFO NPs

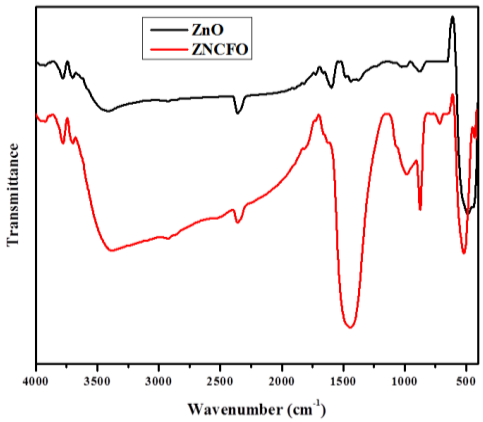

Fig. 4 – FT-IR spectra of pure ZnO and ZnNiCaFeO NPs

The emission spectra of the ZnO NPs with six peaks at 386, 395, 410, 459 and 488 nm are defined. The emission spectra observed at 380 and 395 nm range (band to band transition at UV region) are mainly attributed to radiative recombination of the free exciton-exciton collision [14], 410 nm (violet emission) electron transition from a shallow donor level of the natural zinc interstitials to the top level of the valence band [15], 433 nm (blue emission) singly ionized Zn vacancies and surface defects in the ZnO NPs[16], 459 and 488 nm (blue-green emission) corresponding to the transition between oxygen vacancy and oxygen interstitial defect vacancies [17, 18].

PL emission spectra of ZnNiCaFeO NPs, the red shift is observed compared to ZnO NPs due to various parameters, such as electron phonon coupling, lattice distortion, localization of charge carriers due to interface effects and point defects [19]. A small band shift in

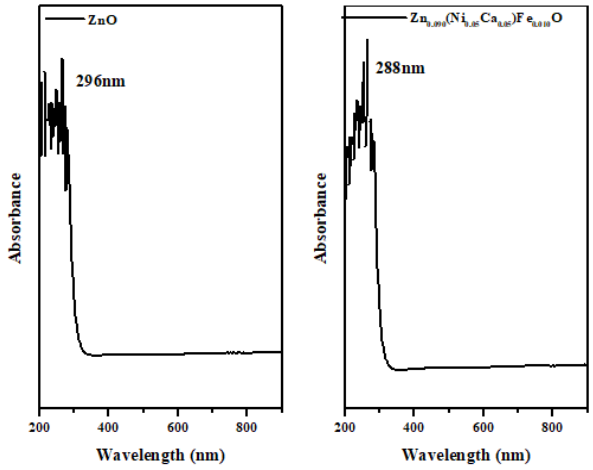

Fig. 5 – UV-Vis spectra of (a) pure ZnO and (b) ZnNiCaFeO NPs

the near band edge (388 nm), violet emission (400 nm), blue emission (438 nm), blue green emission (458 and 498 nm) attributed to the dopant effects. The yellow emission band is observed at 563 nm in ZnNiCaFeO sample due to the presence of interstitial oxygen vacancies [20]. The shift and variation in the emission values confirmed the presence of Ni, Ca and Fe into the ZnO matrix.

In the XRD results of ZNCFO sample, secondary phase might exist due to the presence of Fe^{3+} ion, which is useful to consider all possible ferromagnetic impurity phase present in the sample. Room temperature ferromagnetism is correlated to Fe-related oxide such as Fe_3O_4 or Fe cluster and also the presence of oxygen vacancies will change in the band structure of host semiconductors [24]. In literature, the intrinsic defects play vital role in the ferromagnetism of transition metal doped ZnO and the oxygen vacancies with the trapped occupying an orbital overlapping with the *d* shells of transition metals [25]. In our results, PL spectra of ZNCFO sample, the yellow emission band observed at 563 nm is attributed to the presence of interstitial oxygen vacancies. In case of ZnO NPs, the yellow emissions disappear as compared to ZNCFO sample. The shift and variation in the emission values confirm the presence of metal Ni, Ca and Fe into the ZnO matrix.

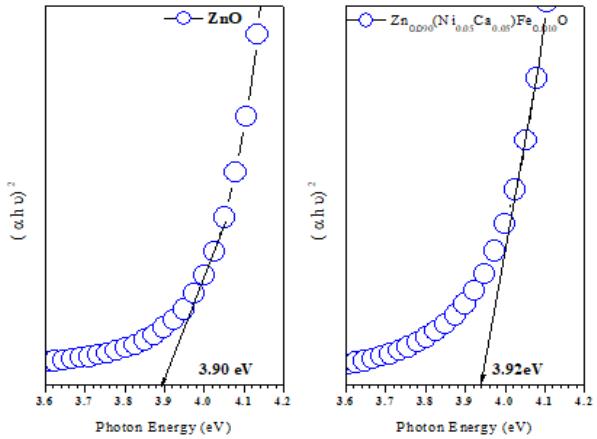

Fig. 6 – Band gap of (a) pure ZnO and (b) ZnNiCaO NPs

4. CONCLUSIONS

The present study is focused on the synthesis of ZnO and ferrite composition ZNCFO using single step co-precipitation method. From the XRD patterns, the synthesized ZnO and ZNCFO NPs exhibits a hexagonal wurtzite structure. FESEM images showed the synthesis ZnO and ZNCFO NPs formed hexagonal rod like structures and nanorods filled with uniform grain boundaries. From the EDX analysis, the chemical compositions were estimated. FT-IR spectra, the various vibrational frequencies were assigned for ZnO and ZNCFO NPs. The band gap increases from 3.91 to 3.92 eV in the doped sample due to the effect of Ni, Ca and Fe doping effects. Room temperature ferromagnetism is correlated to Fe cluster and also the presence of oxygen vacancies in the band structure of host semiconductors.

REFERENCES

1. E. Bacaksiz, M. Parlak, M. Tomakin, A. Özçelik, M. Karakız, M. Altunbaş, *J. Alloy. Compd.* **466** No 1-2, 447 (2008).
2. Jun Wang, Jieming Cao, Baoqing Fang, Peng Lu, Shaogao Deng, Haiyan Wang, *Mater. Lett.* **59** No 11, 1405 (2005).
3. Linping Xu, Yan-Ling Hu, Candice Pelligra, Chun-Hu Chen, Lei Jin, Hui Huang, Shanthakumar Sithambaram, Mark Aindow, Raymond Joesten, Steven L. Suib, *Chem. Mater.* **21** No 13, 2875 (2009).
4. S. Cho, S.-H. Jung, K.-H. Lee, *J. Phys. Chem. C* **112** No 33, 12769 (2008).
5. Panit Chantharasupawong, Reji Philip, Tamio Endo, Jayan Thomas, *Appl. Phys. Lett.* **100** No 22, 221108 (2012).
6. Swapna S. Nair, Jinto Thomas, C.S. Suchand Sandeep, M.R. Anantharaman, Reji Philip, *Appl. Phys. Lett.* **92** No 17, 171908 (2008).
7. Saime Sebnem Cetin, Ibrahim Uslu, Arda Aytimur, Suleyman Ozcelik, *Ceram. Int.* **38** No 5, 4201 (2012).
8. C. Karthikeyan, L Arun, A.H. Hameed, K. Gopinath, L. Umaralikahan, G. Vijayaprasath, P. Malathi, *J. Mater. Sci.: Mater. Electron.* **15** No 9, 8097 (2019).
9. Chao-Ming Fu, Ming-Ru Syue, Fu-Jin Wei, Chao-Wen Cheng, Chan-Shin Chou, *J. Appl. Phys.* **107** No 9, 09A519 (2010).
10. Abdulrahman Syedahamed Haja Hameed, Chandrasekaran Karthikeyan, Seemaisamy Sasikumar, Venugopal Senthil Kumar, Subramanian Kumaresan, G. Ravic, *J. Mater. Chem. B* **1** No 43, 5950 (2013).
11. Nelsa Abraham, Alex Rufus, C. Unni, Daizy Philip, *Mater. Sci.: Mater. Electron.* **28** No 21, 16527 (2017).
12. L. Xiao, S.H. Lie, Z. Hui, L.B. Bin, *Trans. Nonferrous Met. Soc.* **17**, 814 (2007).
13. Y.D. Zenis, *Carbon and Ceramic Nanofibres* (Science Mag. Org.: 2004).
14. Sheo K. Mishra, Rajneesh K. Srivastava, S.G. Prakash, Raghvendra S. Yadav, A.C. Panday, *Opto-Electron. Rev.* **18**, No 4, 467 (2010).
15. Y.W. Heo, D.P. Norton, S.J. Pearton, *J. Appl. Phys.* **98** No 7, 073502 (2005).
16. Lin Bixia, Zhuxi Fu, Yunbo Jia, *Appl. Phys. Lett.* **79** No 7, 943 (2001).
17. Lija Arun, Chandrasekaran Karthikeyan, Daizy Philip, D. Dhayanithi, N.V. Giridharan, C. Unni, *Opt. Quant. Electron.* **50** No 12, 414 (2018).
18. Volker Noack, Alexander Eychmüller, *Chem. Mater.* **14** No 3, 1411 (2002).
19. S. Zhou, K. Potzger, H. Reuther, K. Kuepper, W. Skorupa, M. Helm, J. Fassbender, *J. Appl. Phys.* **101**, 09H109 (2007).

Підготовка та дослідження наночастинок ZnO, легованих Ni, Ca та Fe

Srinivasan Kumar[1], K.K. Sivakumar[2], Naol Dessalegn Dejene[1], Temesgen Garoma[1], Asagid Tadesse[1]

[1] *Wollega University, Nekemte, Ethiopia*
[2] *Academy of Maritime Education and Training Deemed to be University, India*

Наноструктури оксидів металів відіграють важливу роль у визначенні магнітних, оптичних та електричних характеристик. У роботі були підготовлені наноструктуровані композити на основі ZnO та вивчені їх магнітні та оптичні властивості. Підготовлений композит має склад $Zn_{0.09}(Ni_{0.05}Ca_{0.05})Fe_{0.01}O$ (ZnNiCaFeO) і отримується методом співосадження з подальшим спіканням. Щоб розрізнити роль композитів, також готують чистий ZnO, а його властивості порівнюють із характеристиками композитних матеріалів. Обидва ZnNiCaFeO демонстрували гексагональну структуру типу вюрцит з розміром зерна близько 52 нм та 46 нм. Структуровану морфологію гексагональних нанострижнів та атомну концентрацію підготовлених композитів визначено відповідно за допомогою FESEM та EDAX. Спектри поглинання зразків (UV-Vis) показали пік поглинання при 296 нм для ZnO та при 288 нм для наночастинок ZnNiCaFeO. Довжина хвилі збудження композиційних матеріалів також оцінюється з досліджень PL. Відзначається, що композитний ZnNiCaFeO демонструє феромагнітну поведінку при великих значеннях намагніченості 0,34914 ему/г. Таким чином, отримані результати вказують на те, що композити можуть бути використані як у додатках магнітом'яких матеріалів, так і в різних оптичних.

Ключові слова: Оксид цинку, Співосадження, Вюрцит, Оптичні властивості, Феромагнітний.